ETH
Eidgenössische Technische Hochschule Zürich
Swiss Federal Institute of Technology Zurich

Institute for Biomechanics

Ishan Kapnadak

Micro-Multiphysics Agent-based Modeling of Human Bone Remodeling: Exploring the Dual Action Effect of Romosozumab

Internship Report

Institute for Biomechanics
Swiss Federal Institute of Technology (ETH) Zurich

Advisors

Charles Ledoux

Supervisor

Prof. Dr. Ralph Müller

September 23, 2022

Acknowledgment

I would like to thank Prof. Dr. Ralph Müller for giving me the opportunity to complete my research internship at the Laboratory for Bone Biomechanics at the Institute for Biomechanics, ETH Zürich. The two months I spent at Zürich have helped me grow immensely as a researcher.

I would like to express my deepest gratitude to my advisor, Charles Ledoux, for his feedback and support at all times. This project would not have been possible without his guidance and advice.

Additionally, I would like to thank Prof. Harry van Lenthe and the CSCS Swiss National Supercomputing Centre for providing me with the necessary computing power required to run my simulations.

I had the immense pleasure of interacting with members of the Laboratory for Bone Biomechanics. I would like to thank each and every member of the lab for welcoming me and making me feel at home. I truly believe that this multicultural and diverse experience has helped me grow as a person.

Finally, I would like to thank my family and friends for supporting me throughout the duration of my internship.

Abstract

Osteoporosis is a bone disorder most prevalent in postmenopausal women, causing the bone to become brittle and weak. It is estimated that one in three women over the age of 50 years suffer a fragility fracture in their remaining lifetime as a result of osteoporosis. Osteoporosis is most commonly treated using anti-resorptive drugs (bisphosphonates, denosumab) and anabolic drugs (PTH, romosozumab).
The aim of this project is to adapt the existing model to simulate the effect of treatment with romosozumab, an anabolic sclerostin inhibitor. Romosozumab is incorporated into the model as an additional cytokine that competes with LRP6 to bind with sclerostin. The model is also modified to incorporate a sclerostin-dependent level of RANKL production.
Simulations are run with monthly subcutaneous injections of 210mg of romosozumab to obtain change in bone formation and bone resorption post romosozumab injection that match bone turnover marker (BTM) measurements in clinical trials. This adapted model is then used to generate 6-month in-silico results for response to treatment with both placebo and romosozumab, on 7 biopsies. These results are then compared to previous results obtained in clinical trials. Finally, the effect of initial biopsy conditions on the response to romosozumab treatment is also analyzed.

Contents

1. Introduction

Osteoporosis is a bone disease characterised by a decrease in bone mass and an increased risk of fragility fractures, most commonly in the hip, wrist, or spine.[1]. An estimated 200 million women are affected by osteoporosis worldwide with more than 8.9 million osteoporotic fragility fractures being reported annually (an osteoporotic fracture every 3 seconds!) [2, 3]. Individuals diagnosed with osteoporosis often suffer from chronic pain, and have a decreased quality of life [1]. This in turn also poses a huge economic burden on society with experts estimating that osteoporotic fractures may cost as high as $25.3 billion annually [4]. It is thus crucial to understand the underlying mechanics of bone remodeling in humans, and to quickly and inexpensively study the efficacy of various treatment options for osteoporosis.

1.1. Background

Postmenopausal women are especially at high risk of osteoporosis[5], with nearly one in three women over the age of 50 years suffering an osteoporotic fragility fracture during their remaining lifetime [3]. In a healthy adult, the process of bone remodeling is steady, with a delicate balance between bone formation by osteoblasts and bone resorption by osteoclasts. [6]. This balance is disturbed in post-menopausal women on account of an estrogen deficiency [5, 6]. Estrogen aids the apoptosis of osteoclasts, and thus a decrease in estrogen results in increased bone turnover and loss of bone. [5, 6]. This interaction between estrogen and osteoclasts is illustrated in Figure 1.1.

Pharmocological therapies commonly prescribed to high fracture risk patients are generally divided into two.

1. Anti-resorptive medication: bisphosphonates, denosumab, etc.
2. Anabolic or dual-action medication: PTH, romosozumab, etc.

Anti-resorptive medications reduce the number of osteoclasts and thus decelerate the process of bone resorption, leading to decreased turnover. This however is less effective in diabetic patients where bone turnover is already low. Thus, anti-resorptive treatment is expected to be less efficient in diabetic patients. This is illustrated in Figure 1.2.
Anabolic medications on the other hand have a dual-active approach, reducing the number of osteoclasts leading to decreased bone resorption, while also increasing the number of osteoblasts leading to increased bone formation. One such example is that of romosozumab, a monoclonal sclerostin antibody. Romosozumab binds to sclerostin, which in turn prevents its inhibitory effect on bone formation. As a result, the Wnt signalling

pathway is activated, leading to increased bone formation. This interaction is illustrated in Figure 1.1. The dual-active effect of romosozumab is illustrated in Figure 1.3

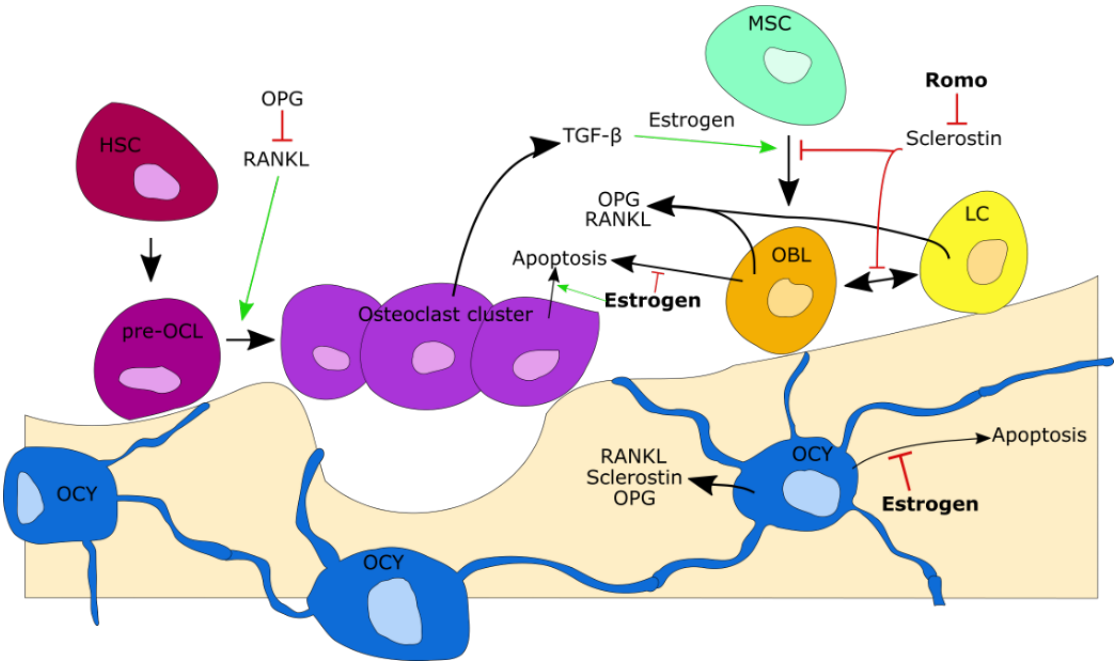

Figure 1.1: Interactions between cells and cytokines during bone remodeling, with the illustration of the mechanism of action of romosozumab in particular. Adapted from Ledoux et al. (2019) [7].

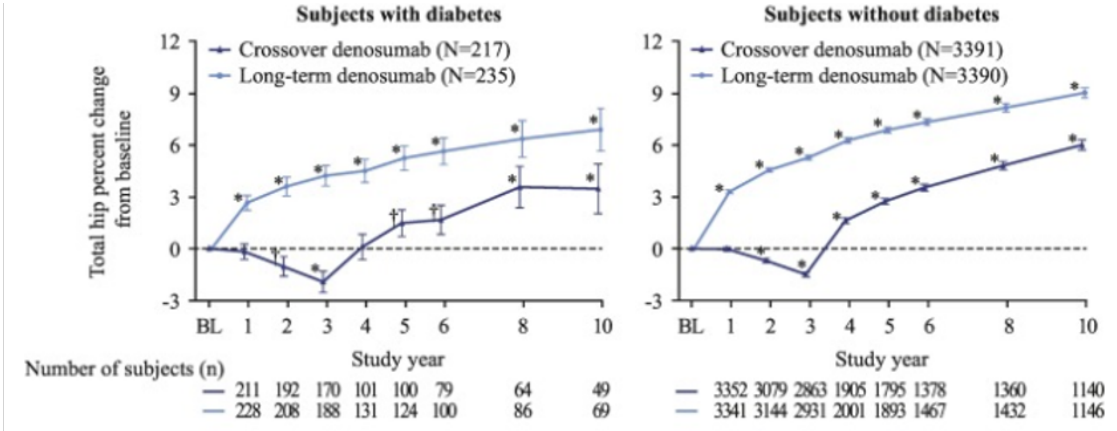

Figure 1.2: Diabetic subgroup of FREEDOM trial had less effective response to anti-resorptive treatment with denosumab. Adapted from

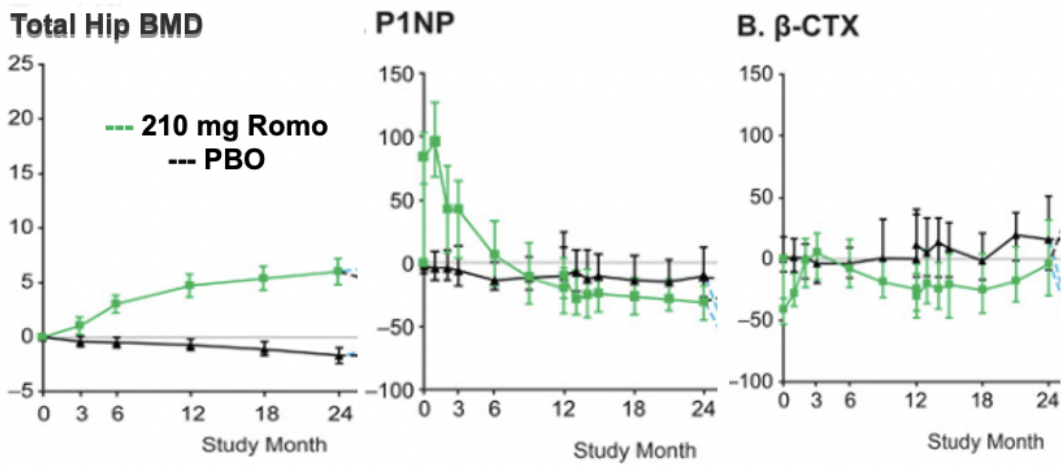

Figure 1.3: The sclerostin antibody romosozumab has a dual-active approach, increasing formation and reducing resorption. Adapted from McClung et al. (2018) [8].

1.2. Motivation and Aim

The need for rapid testing of treatment options for osteoporosis has already been outlined. The process of human bone remodeling, however, is quite slow. Thus, the evaluation of treatment options via experimental studies and clinical trials is both time-consuming and costly. The use of *in silico* models that simulate the process of remodeling at a faster time-scale present a natural, quick, and inexpensive solution to this problem.
Of the various *in silico* models being developed, micro-multiphysics agent-based (micro-MPA) models have proven to be quite popular. Micro-MPA models incorporate the complex cell-cytokine pathways present in bone, and are also able to enable the simulation of disorders like osteoporosis along with the investigation of treatment options. The Laboratory for Bone Biomechanics at ETH Zürich has already developed such a micro-MPA model. The aim of this project is to

- To propose and implement a mechanism to adapt this existing micro-MPA model to obtain changes in bone formation and bone resorption post romosozumab injection that match bone turnover marker (BTM) measurements in clinical trials
- To use this adapted model to generate 6-month *in silico* results for response to treatment with both placebo and romosozumab, on 7 biopsies, and compare the bone mineral density (BMD) trends obtained with previous clinical results
- To analyze the effect of initial biopsy conditions on the response to treatment with romosozumab.

2. Methodology

The following chapter describes the simulation methods for modeling the effect of osteoporosis on bone and its treatment with romosozumab. The environment of the simulation is based on micro-CT images that are digitally extracted, processed, and fed into a micro-MPA model. Chapter 2.1 presents the selection criteria for the micro-CT scans that are used in this study. Chapter 2.2 details the adaptations made to the micro-MPA model for the simulation of treatment with romosozumab.

2.1. Micro-CT Scans

Computational models that simulate bone remodeling (such as the micro-MPA model) often use high-resolution micro-CT images as their input [9]. These images are also commonly used to study bone microstructure, monitor the development of osteoporosis, and investigate its treatment with medication [9]. The baseline micro-CT scans used in this project are taken from the ones selected for the previous ten-year micro-MPA simulation study with denosumab by Tourolle et al. [10]. These scans are based on 7 out of 25 iliac crest biopsies from a group of postmenopausal women with an average age of 72 years that are included in the ETH Zürich biopsy database. These images were acquired at a resolution of 10.5 μm. The samples were selected according to the criteria presented in [10]. The number of ways to choose 7 out of 25 biopsies was reduced to 50 by minimizing a weighted normalized error for each set of 7 biopsies with respect to average BV/TV (%), average age (years), standard deviation of BV/TV (%), standard deviation of age (years), and uniformity of BV/TV increments. This error is shown in Equation 2.1.

$$\text{Error} \quad = \sum_{i=\text{BV/TV, Age, ...}} w_i \cdot \frac{|\text{Set\_point}_i - \text{Value}_i|}{\text{Set\_point}_i} \tag{2.1}$$

Out of these 50 ways, the selected combination of 7 biopsies was the one that most closely matched the average BV/TV of the FREEDOM trial (NCT00089791, registered with ClinicalTrials.gov [11]) [10].

2.2. In Silico Model

Image properties extracted from the biopsies are used to define the environment in the *in silico* model. This project further adapts the *in silico* model by Tourolle and colleagues [10, 12] from the Institute for Biomechanics at the ETH Zürich as detailed in in Chapter 2.2.3.

The model combines (i) a finite element analysis tool, and (ii) an agent-based model. This allows the model to simulate both the mechanics (via (i)) as well as cell population dynamics, production reaction, and diffusion of substances (via (ii)) in bone. The model uses a voxel-based lattice with cells such as osteoblasts and osteoclasts being seeded on this lattice. Each voxel contains only one cell and has dimension 21 μm. The agent-based model allows each cell within the model to act as an independent agent. Each agent senses its local environment (mechanical signals and cytokine concentrations), and responds by either forming or resorbing bone, and producing biomolecules. [10]

2.2.1. Finite Element Analysis

Bone remodelling in response to mechanical stimuli is simulated via the application of an actual load. [13]. This is followed by the use of finite element analysis and a load estimation algorithm to obtain the resulting boundary conditions for each biopsy. BMD is extracted and converted to a Young's Modulus for each voxel using a linear conversion (Mulder et al. [14]). A Parallel Octree Solver (ParOSol) is used to solve for the local mechanical signal. [15].

2.2.2. Agent-Based Model

All biological interactions during the bone remodelling process are managed by the agent-based model. Parameters relevant to cell and cytokine behavior are set based on Ledoux et al. [16] *(unpublished)*. Osteoblasts are placed at high-strain and osteoclasts at low-strain locations, as prescribed in [10]. Placebo data in the FREEDOM trial is used to set the initial cell density of osteoblasts and osteoclasts. Mesenchymal and hematopoietic stem cells (MSC and HSC) are seeded at a density of 8'000 cells/mm^3 in the marrow. The number of osteocytes in the bone matrix is set to 4'800 cells/mm^3 [10].

2.2.3. Adaptations to the Simulation Model

Romosozumab is incorporated into the model as an additional cytokine named "romo". The cytokine "romo" is modeled to bind reversibly with sclerostin to form a complex designated "romosclerostin", as shown in Equation 2.2

$$\text{romo} + \text{sclerostin} \underset{\text{k}_{\text{off}}}{\overset{\text{k}_{\text{on}}}{\rightleftharpoons}} \text{romosclerostin} \tag{2.2}$$

The reaction constants k_{on} and k_{off} are set to . Romosozumab competes with LRP6, both of which bind to sclerostin. The reaction of LRP6 with sclerostin is shown below in Equation 2.3 with $k_{\text{on}} = 0.02$ and $k_{\text{off}} = 10^{-3}$.

$$\text{LRP}_6 + \text{sclerostin} \underset{\text{k}_{\text{off}}}{\overset{\text{k}_{\text{on}}}{\rightleftharpoons}} \text{LRP}_6\text{−sclerostin} \tag{2.3}$$

The model is set up to simulate monthly subcutaneous injections of 210mg of romosozumab as prescribed by phase 1 of clinical trials.

Production of RANKL by osteoblasts and osteoclasts is dependent on the level of sclerostin binding. The level of RANKL production is low when sclerostin binding is low and the number of LRP6 free sites is high. The model is also adapted to include this dependence of RANKL production on sclerostin binding. The rate of RANKL production is characterized in terms of the ratio of free LRP6 sites to occupied LRP6 sites. This ratio is mapped to the rate of RANKL production via an exponential function, as shown in Equation 2.4

$$\text{Rate of RANKL production} \ = e^{-ax} \tag{2.4}$$

where x denotes the ratio of free LRP6 sites to occupied LRP6 sites. When the ratio of free to occupied LRP6 sites is close to 0, the number of LRP6 free sites is very low, and thus the sclerostin level is high. As a result, the rate of RANKL production is high. On the other hand, when the ratio of free to occupied LRP6 sites is close to ∞, the number of LRP6 free sites is very high, and thus the sclerostin level is low. As a result, the rate of RANKL production is low. The hyperparameter a controls how quickly the rate of production decays as sclerostin drops. Figure 2.4 illustrates the effect of varying a on the rate of RANKL production.

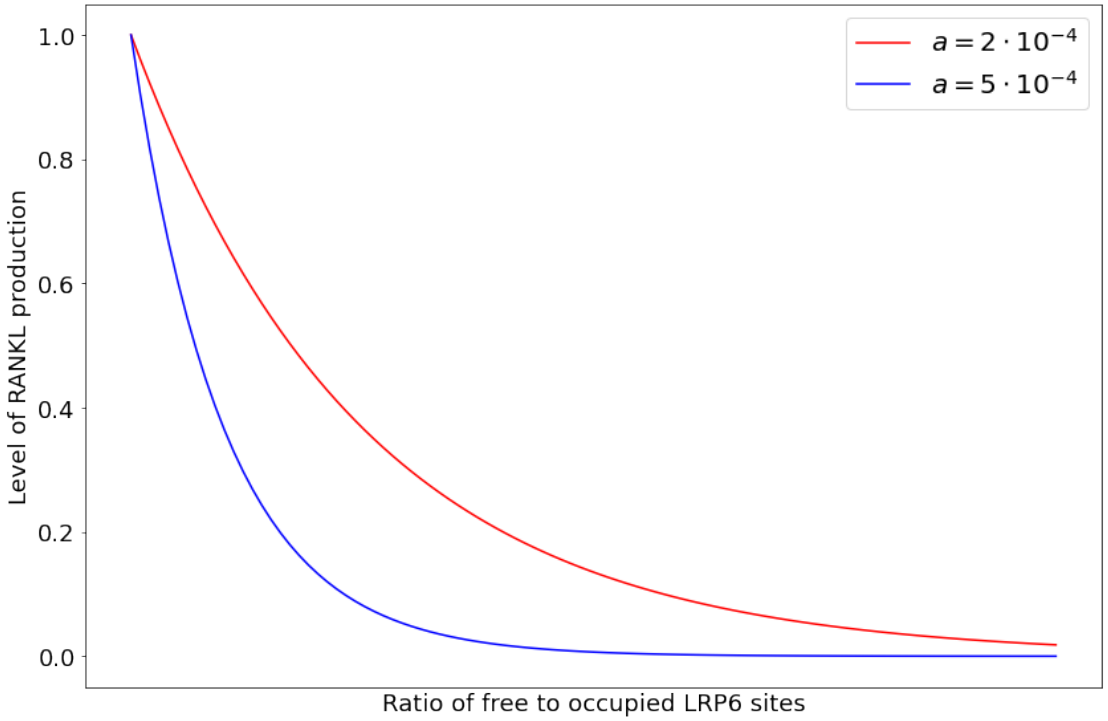

Figure 2.1: When the decay rate a is high, the rate of RANKL production decays quickly as the level of sclerostin drops. On the other hand, when the decay rate a is low, the rate of RANKL production decays much slower as the level of sclerostin drops.

A sensitivity study on this decay rate was carried out, with $a = 2 \cdot 10^{-4}$ proving to give good results.

2.2.4. Temporal Setup

Simulations of treatment with romosozumab are run in time-lapse for a duration of 1 to 6 months. The biopsies on which the simulations are run have an average age of 72 ± 5 years, and monthly subcutaneous injections of romosozumab are administered. The first romosozumab injection is not administered until the 20^{th} day to observe the stable remodeling state before clinical intervention.

3. Results

3.1. Cell and Cytokine Behaviour post Romosozomab Injection

Simulations of one month were run to verify if the model implemented behaves as expected. During this one-month period, 210mg of romosozumab is injected subcutaneously exactly once on the 20^{th} day. Treatment with placebo is also simulated for comparison.

Bone mineral density immediately starts to rise sharply post romosozumab injection due to an increase in bone formation, as expected. On the other hand, no significant change takes place bone mineral density when treated with placebo. This is illustrated in Figure 3.1.
Sclerostin levels drop sharply post romosozumab injection, as expected, since romosozumab binds with sclerostin leading to a sharp drop in sclerostin concentration. On the other hand, sclerostin levels barely change on treatment with placebo since there is no romosozumab to bind with sclerostin. This is illustrated in Figure 3.2.
The number of osteoblasts increase sharply post romosozumab injection, since romosozumab binds to sclerostin preventing its inhibitory effect on formation. With placebo, however, this effect is not seen and the number of osteoblasts do not increase. This is illustrated in Figure 3.3.
The number of osteoclasts stop increasing post romosozumab injection, with a slight drop. In case of treatment with placebo, the number of osteoclasts continues to increase. This is illustrated in Figure 3.4.

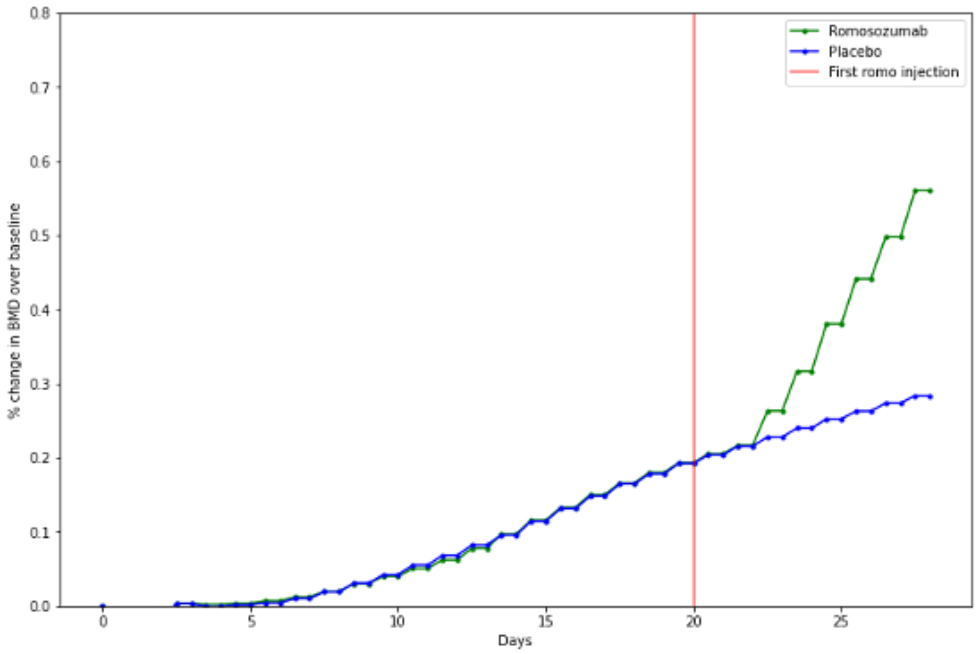

Figure 3.1: Effect of romosozumab injection on bone mineral density.

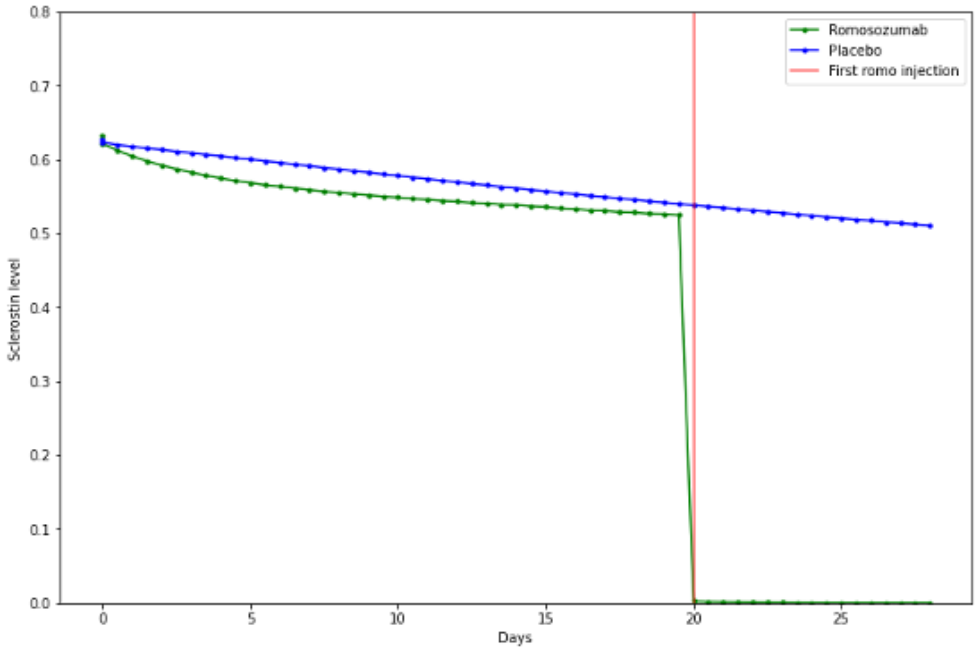

Figure 3.2: Effect of romosozumab injection on sclerostin level.

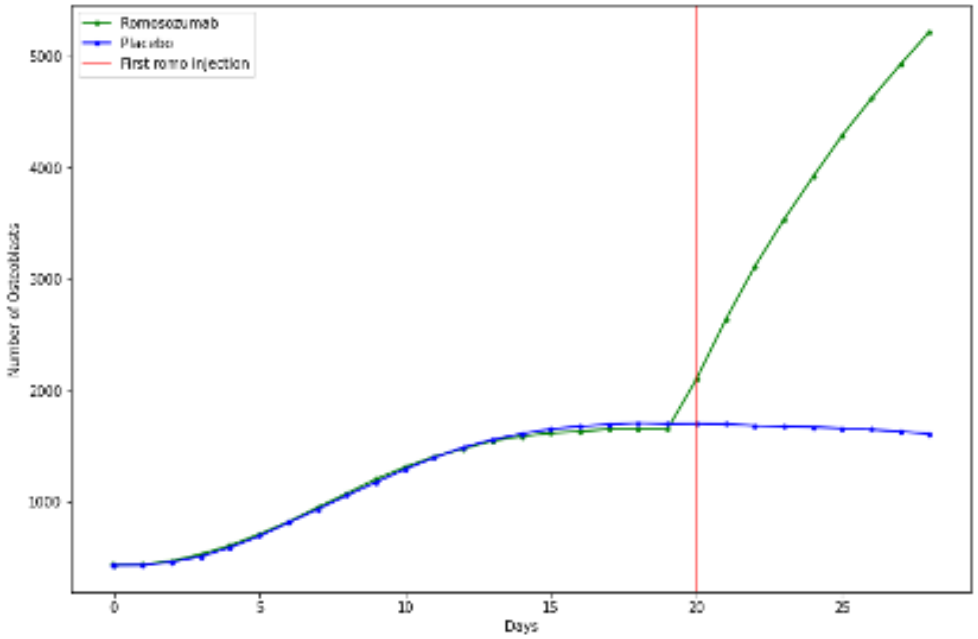

Figure 3.3: Effect of romosozumab injection on the number of osteoblasts.

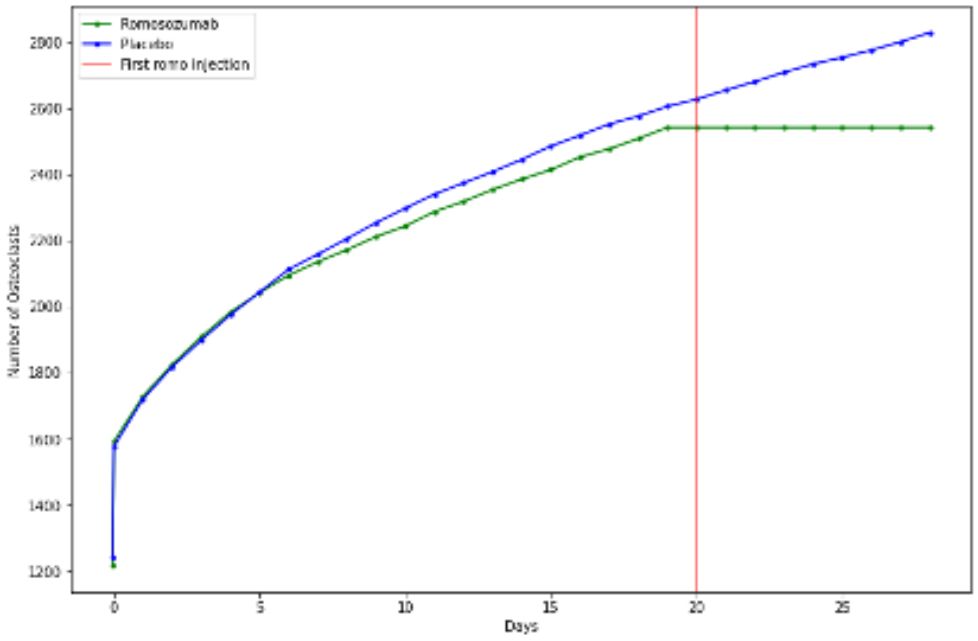

Figure 3.4: Effect of romosozumab injection on the number of osteoclasts.

3.2. Trends in Bone Mineral Density Changes over Time

Once the model was adapted, simulations were run for a duration of 6 months for treatment with both romosozumab and placebo. 210mg of romosozumab was injected subcutaneously every month, as shown in Figure 3.5.

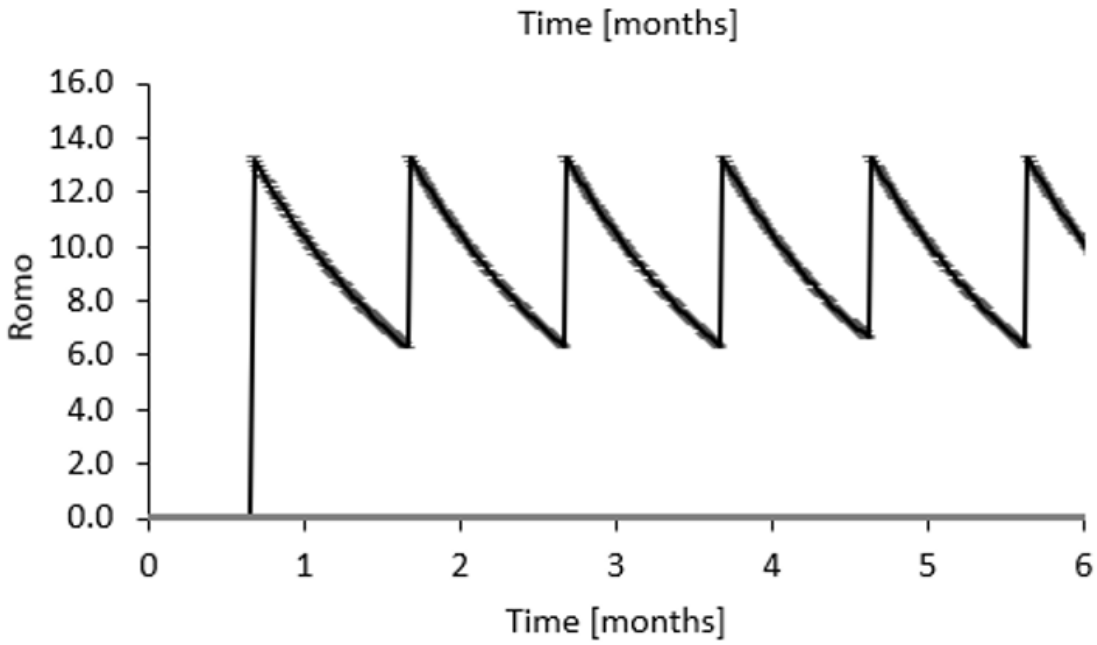

Figure 3.5: Evolution of romosozumab concentration over time, with 210mg of romosozumab being injected subcutaneously every month.

The bone mineral density trends for treatment with both romosozumab and placebo are shown in Figure 3.6. We see that there is no significant change in bone mineral density for the placebo case. With romosozumab, bone mineral density increases substantially and levels off after around 6 months.

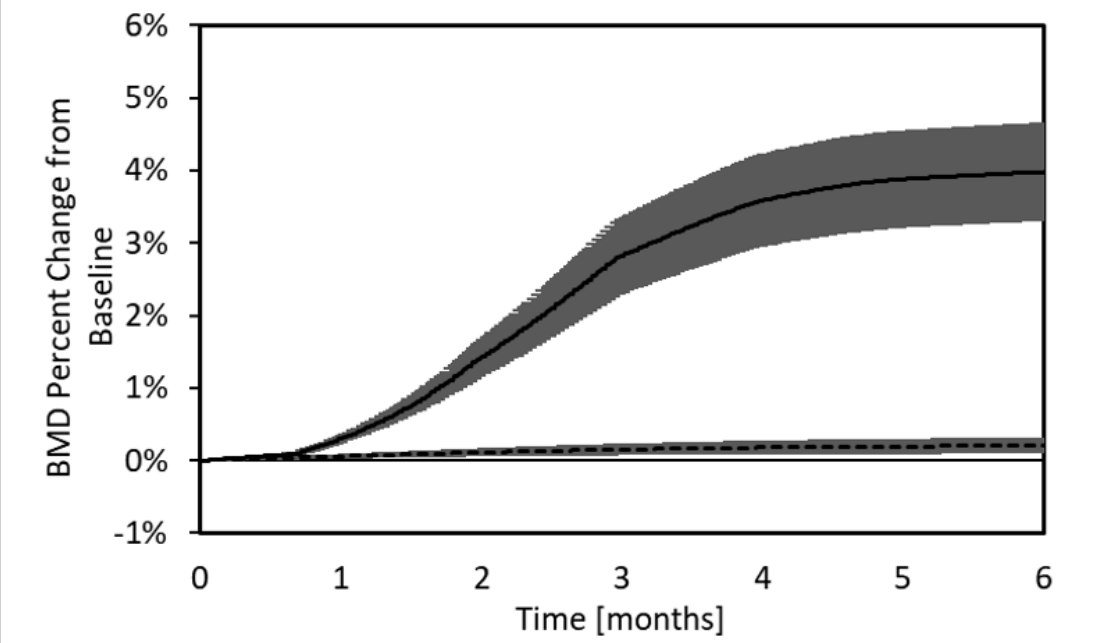

Figure 3.6: Evolution of bone mineral density over time.

3.3. Trends in Cell Numbers over Time

Figures 3.7 and 3.8 show the trends in cell numbers over 8 months during treatment with romosozumab and placebo respectively. We see a sharp increase in osteoblasts and a sharp decrease in osteoclasts on treatment with romosozumab, with no analogous significant changes on treatment with placebo.

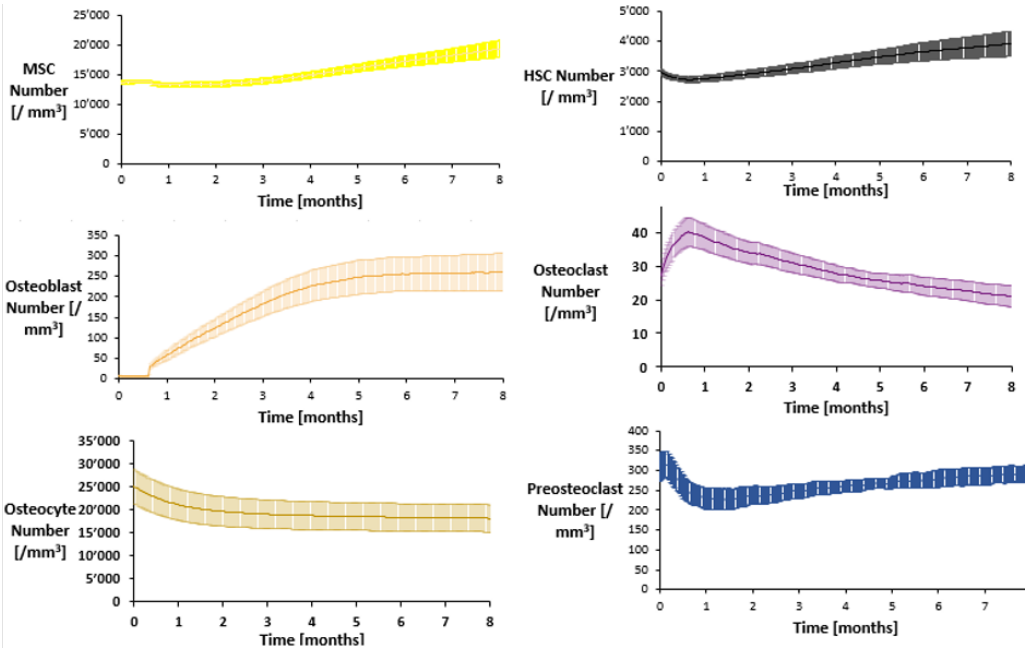

Figure 3.7: Cell number trends for treatment with romosozumab.

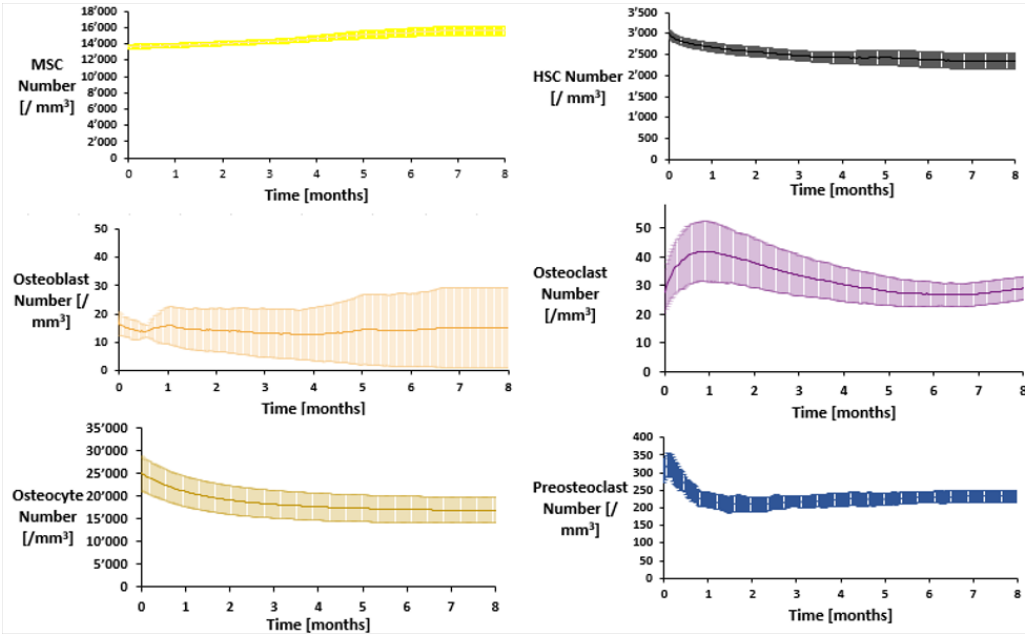

Figure 3.8: Cell number trends for treatment with placebo.

3.4. Effect of Initial Biopsy Conditions on Response to Treatment with Romosozumab

The effect of different initial biopsies on the response to treatment with romosozumab was also examined. In particular, the effect of the initial BV/TV (%) on the evolution of bone mineral density, RANKL, and sclerostin levels was analyzed.

Bone mineral density trends for different biopsies are shown below in Figure 3.9. As expected, the biopsy with the lowest initial BV/TV (%) (BV/TV = 6.8%) shows the highest percentage increase in BMD, whereas the biopsy with higher initial BV/TVs (%) (BV/TV = 21.4% and BV/TV = 15.7%) show low percentage increase in BMD.

Trends in sclerostin level for different biopsies are shown below in Figure 3.10. In all cases, the level of sclerostin rises up until the first romosozumab injection, and then drops sharply. The biopsy with the highest BV/TV (%) (BV/TV = 21.4%) shows extremely high levels of sclerostin.

Trends in RANKL level for different biopsies are shown below in Figure 3.11. In all cases, the level of RANKL rises up until each romosozumab injection after which it drops sharply. No particular conclusion could be drawn regarding how the initial BV/TV (%) affect the level of RANKL.

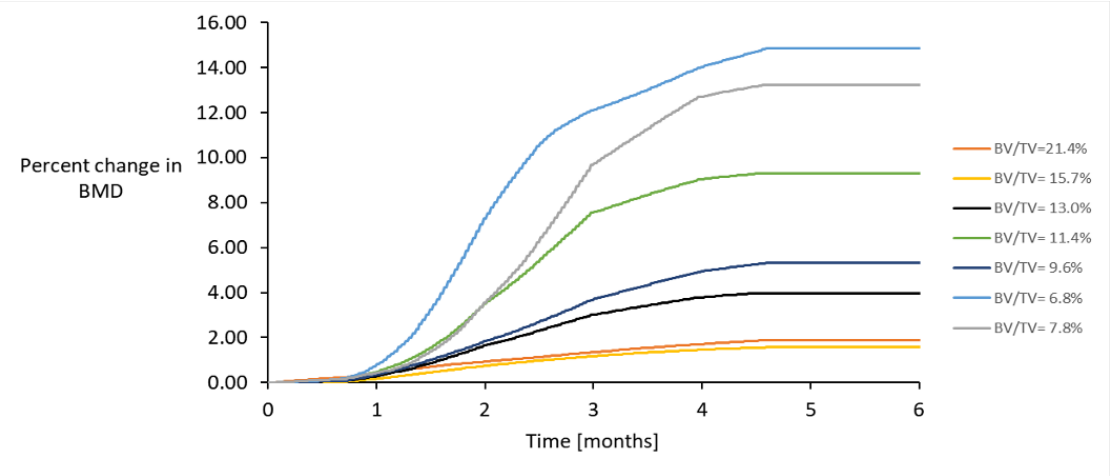

Figure 3.9: Effect of initial BV/TV (%) conditions on the bone mineral density trends.

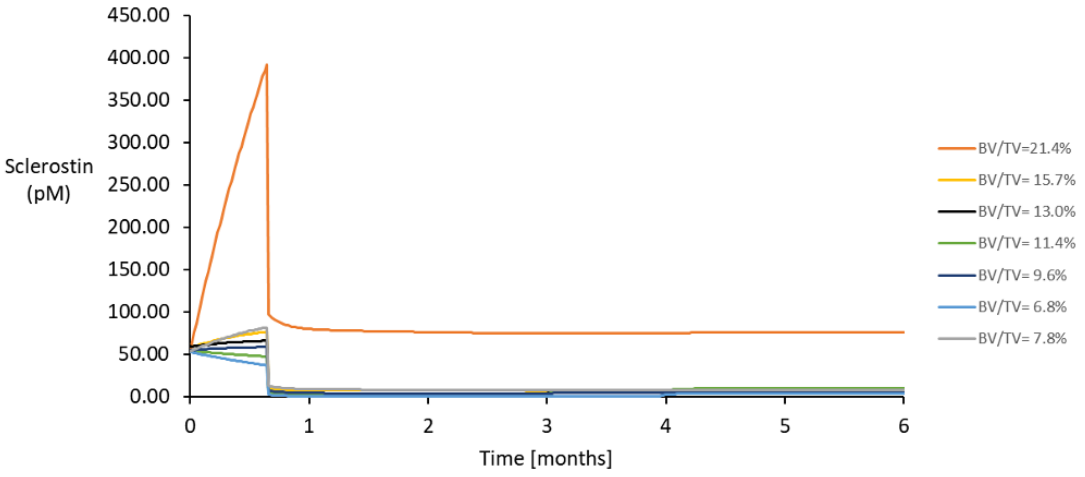

Figure 3.10: Effect of initial BV/TV (%) conditions on sclerostin level trends.

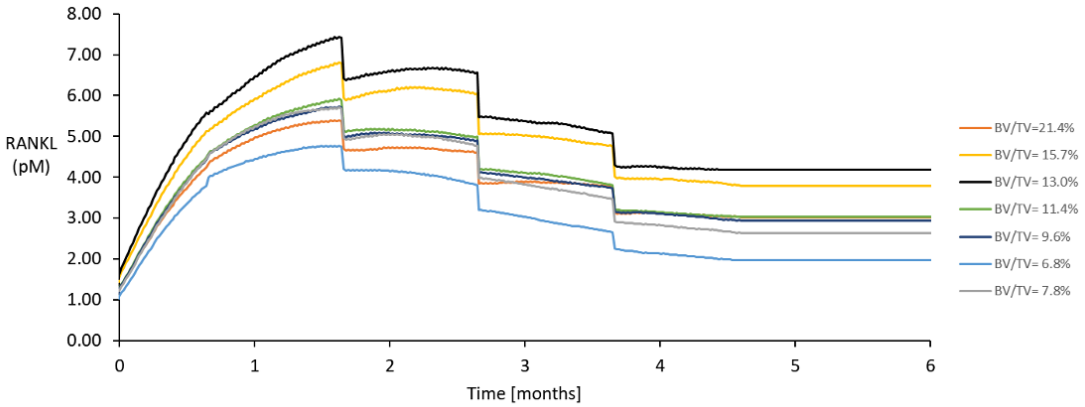

Figure 3.11: Effect of initial BV/TV (%) conditions on RANKL level trends.

4. Discussion, Limitations, and Future Work

As part of this project, treatment with romosozumab was implemented in the existing micro-MPA model. As presented in Chapter 3.1, the behaviour of cells and cytokines immediately post romosozumab injection matched closely with trends seen in clinical trials, with bone mineral density increasing sharply, sclerostin levels dropping sharply, osteoblasts increasing sharply, and osteoclasts dropping slightly. Moreover, Chapter 3.2 indicates a strong rise in bone mineral density with levelling off as expected. The effect of romosozumab injection on RANKL and sclerostin levels are also as expected, as demonstrated in Chapter 3.4. These results suggest significant potential for treatment with romosozumab (and with anabolic agents in general) in patients with diabetes mellitus.

The current model is limited by the small sample size of 7 biopsies, with the possibility of large inter-patient variability. Including more biopsies in the study would allow for further validation of the model. The model does not incorporate certain other pathways that are thought to play essential roles in bone remodeling, especially in diabetic patients, such as inflammatory pathways via interleukins. These can be incorporated into the model as part of a future study to simulate the process of bone remodeling more accurately.

Regarding the bone mineral density trends observed, one limitation is that although the BMD levels off as expected, this levelling off occurs much earlier than seen in clinical trials. A sensitivity study on different parameters affecting this levelling off must be carried out in the future to appropriately adapt the model to better emulate clinical results.

As for trends in cell numbers seen in Chapter 3.3, while the osteoblast and osteoclast numbers seem promising, there is not a lot of information about cell numbers in literature to compare these results with. As such, no strong conclusion could be drawn from these trends.

Finally, simulations were only run for 6 months, which is not a sufficient duration to

conclusively validate the model since treatment with romosozumab often takes longer. As part of future work, one may run simulations of durations extending up to 2 or 5 years, to further validate the model. Further, this study has not focused on morphometrics. Future work may focus on quantifying the effect of initial static morphometrics on response to treatment. One may especially look at structure model index (SMI) and surface gradient, as was done for the study of treatment with denosumab.

A. Appendix

A.1. Location of Files

All data created within this internship project is located in:
home/ikapnadak/public/10 Students/2022/Ishan Kapnadak/02_Output

The micro-CT scans of the 7 biopsies are located in:
home/ikapnadak/public/10 Students/2022/Ishan Kapnadak/01_Biopsies

A.2. Code

Constants

/framework/ifb_framework/constants/molecular_masses.py on the branch *ROMO_CSCS*
/framework/ifb_framework/constants/human.py on the branch *ROMO_CSCS*

The file *molecular_masses.py* contains all the molecular masses of the relevant agents in the micro-MPA model. All constants that are related to humans and used in the *in silico* model are listed in the file *human.py*.

Multiphysics Simulations

/framework/src/multiphysics/... on the branch *ROMO_CSCS*

The agent-based model relies crucially on the files on the branch *ROMO_CSCS*:

- `lattice.hpp`
- `lattice.cpp`
- `reactions.hpp`
- `cells.hpp`
- `cells.cpp`

The scripts `lattice.hpp` and `lattice.cpp` define a lattice which contains arrays for cytokine concentrations, concentration gradients, cells, mechanical signals as well as functions that govern mechanics, cell behaviour and reactions.
The following functions from the lattice class are called in the main script `romo.py`:

- `addDiffusiveProperty()` and `bindDiffusion()` to set diffusive properties for agents.
- `createReactionBindingSite()` and `CellMoleculeCompetitveReaction()` to define rate constants for reactions.
- `inser_or_add_concentration()` to set cytokine concentrations.

The scripts `cells.hpp` and `cells.cpp` are used to define properties for cells. In particular, the file `cells.cpp` contains functions for production of cytokines by each cell. This file also contains the implementation of the exponential sclerostin-dependent production of RANKL by osteoblasts and osteoclasts.

Romosozumab Implementation

The following files are relevant for simulation.

- */framework/ifb_framework/projects/multiscale_bone_remodelling/romo/romo.py* on the branch *ROMO_CSCS*
- */framework/ifb_framework/projects/multiscale_bone_remodelling/romo/pbo.py* on the branch *ROMO_CSCS*
- *scratch/snx3000/ikapnada/simhuman/romo*(patient number)*.slurm*
- *scratch/snx3000/ikapnada/simhuman/pbo*(patient number)*.slurm*
- *scratch/snx3000/ikapnada/parosol_server/launcher.slurm*

The script `romo.py` contains the implementation of treatment with romosozumab. The script `pbo.py` contains the implementation of treatment with placebo. The scripts `romo`(patient number)`.slurm` and `pbo`(patient number)`.slurm` implement the above python scripts on specific input biopsies and queue the jobs to the remote CSCS server. The script `launcher.slurm` launches the parosol server remotely.

A.3. List of Abbreviations

BMD	[–]	Bone Mineral Density
BTM	[–]	Bone Turnover Markers
BV/TV	[–]	Bone Volume over Total Volume
CSCS	[–]	Swiss National Supercomputing Center
FE	[–]	Finite Element
FREEDOM	[–]	Fracture REduction Evaluation of Denosumab for Osteoporosis every 6 Months
HSC	[–]	Hematopoietic Stem Cell
LBB	[–]	Laboratory for Bone Biomechanics

Micro-MPA	[−]	Micro-multiphysics agent-based
MSC	[−]	Mesenchymal Stem Cell
N.Ob	[−]	Osteoblast Number
N.Oc	[−]	Osteoclast Number
OBL	[−]	Osteoblasts
OCL	[−]	Osteoclasts
P1NP	[−]	Procollagen type I N-terminal Propeptide
RANKL	[−]	Receptor Activator of Nuclear factor $\varkappa$ β Ligand
TGF-β	[−]	Transforming Growth Factor β

List of Figures

References

[1] A Svedbom, M Ivergård, E Hernlund, René Rizzoli, and John A Kanis. "Epidemiology and economic burden of osteoporosis in Switzerland". In: *Archives of osteoporosis* 9.1 (2014), pp. 1–8. DOI: https://doi.org/10.1007/s11657-014-0187-y.

[2] Paola Pisani, Maria Daniela Renna, Francesco Conversano, Ernesto Casciaro, Marco Di Paola, Eugenio Quarta, Maurizio Muratore, and Sergio Casciaro. "Major osteoporotic fragility fractures: Risk factor updates and societal impact". In: *World journal of orthopedics* 7.3 (2016), p. 171. DOI: DOI:10.5312/wjo.v7.i3.171.

[3] International Osteoporosis Foundation. *Epidemiology of osteoporosis and fragility fractures*. Accessed June 4, 2022. 2022. URL: https://www.osteoporosis.foundation/facts-statistics/epidemiology-of-osteoporosis-and-fragility-fractures.

[4] V. Muralikrishnan. "(2022". In: *May 5). Osteoporosis Awareness Month 2022. American Society for Biochemistry and Molecular Biology. Retrieved September* 23 (2022).

[5] Richard Eastell, Terence W O'Neill, Lorenz C Hofbauer, Bente Langdahl, Ian R Reid, Deborah T Gold, and Steven R Cummings. "Postmenopausal osteoporosis". In: *Nature reviews Disease primers* 2.1 (2016), pp. 1–16. DOI: https://doi.org/10.1038/nrdp.2016.69.

[6] Meng-Xia Ji and Qi Yu. "Primary osteoporosis in postmenopausal women". In: *Chronic diseases and translational medicine* 1.01 (2015), pp. 9–13. DOI: 10.1016/j.cdtm.2015.02.006.

[7] C Ledoux, D Touralle, D Boaretti, and R Müller. "Cell-scale simulations of bone tissue: micro-multi-physics modelling of osteoporosis and its treatments." Unpublished, 2019.

[8] Michael R McClung, Jacques P Brown, Adolfo Diez-Perez, Heinrich Resch, John Caminis, Paul Meisner, Michael A Bolognese, Stefan Goemaere, Henry G Bone, Jose R Zanchetta, Judy Maddox, Sarah Bray, and Andreas Grauer. "Effects of 24 Months of Treatment With Romosozumab Followed by 12 Months of Denosumab or Placebo in Postmenopausal Women With Low Bone Mineral Density: A Randomized, Double-Blind, Phase 2, Parallel Group Study". In: *Journal of Bone and Mineral Research* 33.8 (2018), pp. 1397–1406. DOI: https://doi.org/10.1002/jbmr.3452. eprint: https://asbmr.

onlinelibrary.wiley.com/doi/pdf/10.1002/jbmr.3452. URL: https://asbmr.onlinelibrary.wiley.com/doi/abs/10.1002/jbmr.3452.

[9] Giulia Molino, Giorgia Montalbano, Carlotta Pontremoli, Sonia Fiorilli, and Chiara Vitale-Brovarone. "Imaging Techniques for the Assessment of the Bone Osteoporosis-Induced Variations with Particular Focus on Micro-CT Potential". In: *Applied Sciences* 10.24 (2020), p. 8939. DOI: https://doi.org/10.3390/app10248939.

[10] Duncan C Tourolle, David W Dempster, Charles Ledoux, Daniele Boaretti, Mauricio Aguilera, Najma Saleem, and Ralph Müller. "Ten-Year Simulation of the Effects of Denosumab on Bone Remodeling in Human Biopsies". In: *JBMR plus* 5.6 (2021), e10494. DOI: https://doi.org/10.1002/jbm4.10494.

[11] ClinicalTrials.gov National Library of Medicine. *A Study to Evaluate Denosumab in the Treatment of Postmenopausal Osteoporosis FREEDOM (Fracture REduction Evaluation of Denosumab in Osteoporosis Every 6 Months), ClinicalTrials.gov Identifier: NCT00089791.* Accessed July 25, 2022. 2014. URL: https://www.clinicaltrials.gov/ct2/show/NCT00089791.

[12] Duncan Tourolle. "A micro-scale multiphysics framework for fracture healing and bone remodelling". PhD thesis. ETH Zurich, 2019. DOI: https://doi.org/10.3929/ethz-b-000364637.

[13] Patrik Christen, Keita Ito, Andreia Andrade dos Santos, Ralph Mller, and Bert van Rietbergen. "Validation of a bone loading estimation algorithm for patient-specific bone remodelling simulations". In: *Journal of Biomechanics* 46.5 (2013), pp. 941–948. ISSN: 0021-9290. DOI: https://doi.org/10.1016/j.jbiomech.2012.12.012. URL: https://www.sciencedirect.com/science/article/pii/S0021929012007427.

[14] Lars Mulder, Jan Harm Koolstra, Jaap MJ den Toonder, and Theo MGJ van Eijden. "Intratrabecular distribution of tissue stiffness and mineralization in developing trabecular bone". In: *Bone* 41.2 (2007), pp. 256–265. DOI: https://doi.org/10.1016/j.bone.2007.04.188.

[15] Cyril Flaig. "A highly scalable memory efficient multigrid solver for μ-finite element analyses". PhD thesis. ETH Zurich, 2012. DOI: https://doi.org/10.3929/ethz-a-007613965.

[16] C Ledoux, D Boaretti, A Sachan, C Collins, and R Müller. "Clinical Data for Verification and Parametrization of Multiphysics Simulations of Post Menopausal Osteoporosis and its Treatments: A Systematic Review of Literature." Unpublished, 2021.